RSC Advances

PAPER

View Article Online
View Journal | View Issue

Cite this: *RSC Adv.*, 2019, **9**, 18359

Induction of cell cycle arrest and apoptosis by copper complex $Cu(SBCM)_2$ towards oestrogen-receptor positive MCF-7 breast cancer cells†

Jhi Biau Foo,*[ab] Li Shan Ng,[a] Ji Hui Lim,[a] Pau Xien Tan,[a] Yan Zhi Lor,[a] Jason Siau Ee Loo,[b] May Lee Low,[c] Lee Chin Chan,[d] Chaw Yee Beh,[e] Sze Wei Leong,[d] Latifah Saiful Yazan,[gh] Yin Sim Tor*[f] and Chee Wun How[a]

Copper complexes have the potential to be developed as targeted therapy for cancer because cancer cells take up larger amounts of copper than normal cells. Copper complex $Cu(SBCM)_2$ has been reported to induce cell cycle arrest and apoptosis towards triple-negative breast cancer cells. Nevertheless, its effect towards other breast cancer subtypes has not been explored. Therefore, the present study was conducted to investigate the effect of $Cu(SBCM)_2$ towards oestrogen-receptor positive MCF-7 breast cancer cells. Growth inhibition of $Cu(SBCM)_2$ towards MCF-7 and human non-cancerous MCF-10A breast cells was determined by MTT assay. Morphological changes of $Cu(SBCM)_2$-treated-MCF-7 cells were observed under an inverted microscope. Annexin V/PI apoptosis assay and cell cycle analysis were evaluated by flow cytometry. The expression of wild-type p53 protein was evaluated by Western blot analysis. The intracellular ROS levels of MCF-7 treated with $Cu(SBCM)_2$ were detected using DCFH-DA under a fluorescence microscope. The cells were then co-treated with $Cu(SBCM)_2$ and antioxidants to evaluate the involvement of ROS in the cytotoxicity of $Cu(SBCM)_2$. Docking studies of $Cu(SBCM)_2$ with DNA, DNA topoisomerase I, and human ribonucleotide reductase were also performed. The growth of MCF-7 cells was inhibited by $Cu(SBCM)_2$ in a dose-dependent manner with less toxicity towards MCF-10A cells. It was found that $Cu(SBCM)_2$ induced G_2/M cell cycle arrest and apoptosis in MCF-7 cells, possibly *via* a p53 pathway. Induction of intracellular ROS was not detected in MCF-7 cells. Interestingly, antioxidants enhance the cytotoxicity of $Cu(SBCM)_2$ towards MCF-7 cells. DNA topoisomerase I may be the most likely target that accounts for the cytotoxicity of $Cu(SBCM)_2$.

Received 26th April 2019
Accepted 3rd June 2019

DOI: 10.1039/c9ra03130h

rsc.li/rsc-advances

1. Introduction

Cancer is a polygenic and multifactorial complex series of disease characterised by an uncontrolled proliferation of cells.[1,2] For the past 50 years, drug treatment for oestrogen-receptor (ER) positive breast cancer has shown great clinical advances and has served as a paradigm for the development of cancer targeted therapies. ER positive is the major subtype of breast cancer, and it has been proven that five years of therapy with tamoxifen reduces the recurrence of breast cancer and improves the overall survival of women with early-stage ER positive breast cancer.[3,4]

Despite the standard regimen with tamoxifen, long term side effects of tamoxifen have been reported. In both Adjuvant Tamoxifen: Longer Against Shorter (ATLAS) trial and the trials of 5 years of tamoxifen *versus* no treatment, tamoxifen was reported to increase the incidence of developing endometrial cancer in postmenopausal women who have not had a hysterectomy before trial entry.[5] This could be due to the off target effects of tamoxifen towards the organ expressing oestrogen

[a]*Faculty of Pharmacy, MAHSA University, Jalan SP2, Bandar Saujana Putra, 42610 Jenjarom, Kuala Langat, Selangor, Malaysia. E-mail: foojhibiau@gmail.com*
[b]*School of Pharmacy, Faculty of Health & Medical Sciences, Taylor's University, No. 1 Jalan Taylor's, 47500 Subang Jaya, Selangor Darul Ehsan, Malaysia. E-mail: JhiBiau.Foo@taylors.edu.my*
[c]*Department of Pharmaceutical Chemistry, School of Pharmacy, International Medical University, No. 126, Jalan Jalil Perkasa 19, 57000 Bukit Jalil, Kuala Lumpur, Malaysia*
[d]*Virology Lab 1, Faculty of Biotechnology and Biomolecular Sciences, Universiti Putra Malaysia (UPM), 43400 Serdang, Selangor, Malaysia*
[e]*Laboratory of Vaccines and Immunotherapeutics, Institute of Bioscience, Universiti Putra Malaysia (UPM), 43400 Serdang, Selangor, Malaysia*
[f]*School of Biosciences, Faculty of Health & Medical Sciences, Taylor's University, No. 1 Jalan Taylor's, 47500 Subang Jaya, Selangor Darul Ehsan, Malaysia. E-mail: YinSim.Tor@taylors.edu.my*
[g]*Laboratory of Molecular Biomedicine, Institute of Bioscience, Universiti Putra Malaysia, 43400 UPM Serdang, Selangor, Malaysia*
[h]*Department of Biomedical Sciences, Faculty of Medicine and Health Sciences, Universiti Putra Malaysia (UPM), 43400 Serdang, Selangor, Malaysia*

† Electronic supplementary information (ESI) available. See DOI: 10.1039/c9ra03130h

receptors. Therefore, it is crucial to discover new strategy to treat oestrogen receptors breast cancer.

Copper is an essential component needed in appropriate amounts for multiple biological processes within the body. However, abnormal elevated levels of copper can be found in cancer tissues in comparison to normal cells.[6] Based on this discovery, our group is developing copper complex to deliver anticancer agent into cancer cells.[7] The increased uptake of copper-anticancer agent complex by cancer cell will increase the selectivity and activity of the anticancer agent. Our previous publication reported that *S*-benzyldithiocarbazate and 3-acetylcoumarin [$Cu(SBCM)_2$] induced cell cycle arrest and apoptosis towards MDA-MB-231 triple-negative breast cancer cell.[8] Nevertheless, its effect towards other breast cancer subtype has not been established. Therefore, the present study was conducted to investigate the effect of $Cu(SBCM)_2$ towards oestrogen-receptor positive MCF-7 breast cancer cells.

2. Material and methods

2.1 Chemicals

Dimethyl sulfoxide (DMSO), ethanol, acetonitrile and pentane were purchased from Friedemann Schmidt (Frankfort, Germany). 3-Acetylcoumarin, dichlorodihydrofluorescein diacetate (DCFH-DA), α-tocopherol (vitamin E), *N*-acetylcysteine (NAC), hydrogen peroxide (H_2O_2), doxorubicin, propidium iodide, RNAse A, bromophenol blue and glycerol were purchased from Sigma-Aldrich (St Louis, MO, USA). Copper(II) acetatemonohydrate was purchased from HmbG Chemicals (Hamburg, Germany). Phenol-red-free RPMI-1640 with L-glutamine, bovine serum albumen (BSA), dulbecco Modified Eagle Medium (DMEM) F12 and Chemi-Lumi One L were purchased from Nacalai Tesque (Kyoto, Japan). Foetal bovine serum, trypsin–EDTA (1×) and penicillin–streptomycin (100×) were purchased from PAA Laboratories (Pasching, Austria). MTT [3-(4,5-dimethylthiazol-2-yl)-2,5-diphenyltetrazolium bromide] was purchased from PhytoTechnology Laboratories (Kansas, USA). Sodium deoxycholate, Triton-X 100 and sodium chloride (NaCl) were purchased from Merck (Darmstadt, Germany). Phenylmethanesulfonyl fluoride (PMSF) and protease inhibitor cocktails were purchased from Calbiochem (San Diego, CA, USA). Sodium dodecyl sulphate (SDS), tris-base, glycine, acrylamide, bisacrylamide, ammonium persulfate (APS), tetramethylethylenediamine (TEMED), 10% Tween-20, Bradford reagent, 2-mercaptoethanol, extra thick blotting paper and pre-stained protein marker were purchased from Bio-Rad (California, USA). Immobilon-FL polyvinylidene fluoride (PVDF) membrane with 0.45 μm pore size was purchased from Millipore (Bedford, MA, USA). Primary mouse antibodies anti-p53 (DO-1: sc-126), anti-beta-actin (sc-47778) and horseradish peroxidase-conjugated anti-mouse (sc-2005) secondary antibodies were purchased from Santa Cruz Biotechnology (CA, USA). Epidermal growth factor (EGF), hydrocortisol, insulin and horse serum were purchased from Life Technologies (Rockville, Maryland). Annexin-V-FITC kits were purchased from BD Bioscience (Singapore).

2.2 Synthesis of copper complex $Cu(SBCM)_2$

$Cu(SBCM)_2$ was prepared and characterised as previously prescribed (Fig. 1).[7] Briefly, *S*-benzyldithiocarbazate was reacted with 3-acetylcoumarin. The mixture was heated for 2–3 hours and allowed to stand for a few hours at 4 °C to afford SBCM-H. $Cu(OAc)_2 \cdot H_2O$ was then added to the SBCM-H solution. The reaction mixture was stirred overnight and concentrated. The precipitate was filtered, washed with pentane and dried under vacuum to afford $Cu(SBCM)_2$ (Fig. 1). Elemental analysis for $C_{38}H_{30}CuN_4S_4O_4$: calcd. C 57.16, H 3.79, N 7.02; found C 56.53, H 3.80, N 7.02. ESI-MS: m/z = $[M + K]^+$ calcd. 836.02, found 836.01; $[M + Na]^+$ calcd. 820.04, found 820.03; $[M + H]^+$ calcd. 798.06, found 798.05. IR: ν (cm^{-1}) = 1726 (s) 1565 (m) 986 (s) 965 (s) 853 (w). The difference between the theoretical and calculated is less than 1%, indicating a high purity of our copper complex $Cu(SBCM)_2$.

2.3 Cell culture

The human oestrogen-receptor positive MCF-7 breast cancer, triple-negative MDA-MB-231 breast cancer and non-cancerous MCF-10A cell lines were purchased from American Type and Culture Collection (ATCC, Manassas, VA, USA). MCF-7 and MDA-MB-231 breast cancer cells were grown in RPMI 1640, supplemented with 10% foetal bovine serum and 1% penicillin–streptomycin (complete growth culture media). MCF-10A cells were cultured in DMEM/F12 supplemented with 10% FBS, 20 ng mL^{-1} epidermal growth factor, 0.5 mg mL^{-1} hydrocortisone, 100 ng mL^{-1} cholera toxin and 10 μg mL^{-1} insulin.

2.4 Determination of cell growth inhibition

MCF-7 cells and MCF-10A were seeded in 96-well plates with 5000 cells per well in 100 μL of complete growth culture media, followed by incubation at 37 °C (5% CO_2 and 95% air) for 24 hours to allow cell attachment. The cells were then treated with $Cu(SBCM)_2$ or tamoxifen for 72 hours. Negative control cells treated with 0.3% DMSO alone was also included. At the end of experiment, MTT (20 μL, 5 mg mL^{-1} in PBS) was added into each well and the plate was incubated for 3 hours. Excess MTT was then aspirated and the formazan crystals formed were dissolved by 150 μL of DMSO. The absorbance, which was proportional to cell viability, was measured at 570 nm and a reference wavelength of 630 nm by using ELx800™ Absorbance Microplate Reader (BioTek Instruments Inc., Vermont,

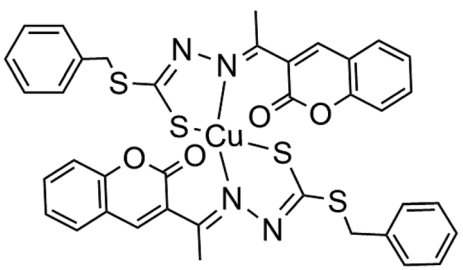

Fig. 1 Copper complex synthesised with *S*-benzyldithiocarbazate and 3-acetylcoumarin [$Cu(SBCM)_2$].

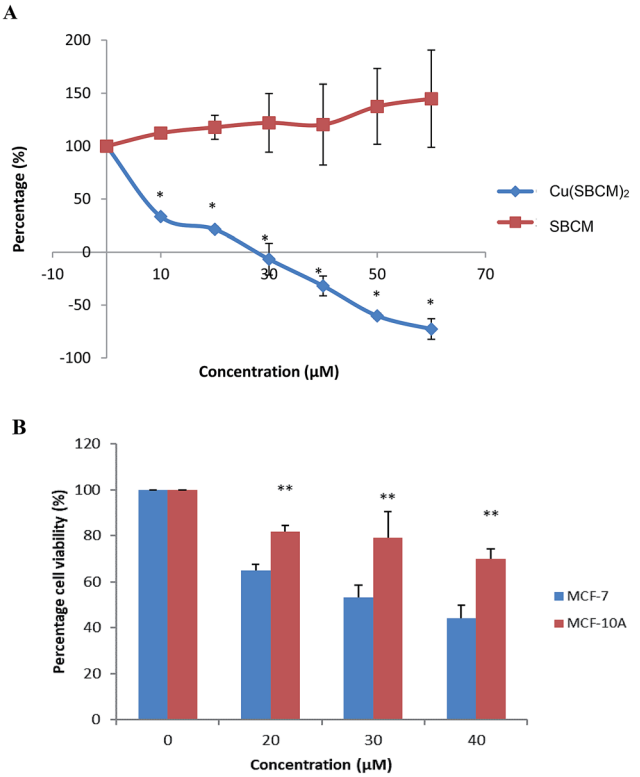

Fig. 2 (A) Effect of SBCM and $Cu(SBCM)_2$ and on the growth of MCF-7 breast cancer cells as determined by MTT assay. * significantly different from the control SBCM at the same concentration ($p < 0.05$). (B) Cell viability of MCF-7 and MCF-10A cells after 48 hours exposure with $Cu(SBCM)_2$. ** indicates $p < 0.05$ when compared between MCF-7 and MCF-10A. Each data point represents the mean of three independent experiments ± SD.

USA). Cell viability was calculated by using formula shown below:

$$\text{Percentage of cell viability}(\%) = \frac{\text{OD}_{570-630}\ \text{treatment}}{\text{OD}_{570-630}\ \text{control}} \times 100\%$$

A graph of percentage of cell growth *versus* concentration of $Cu(SBCM)_2$ was plotted. The concentration of $Cu(SBCM)_2$ which inhibited 50% of cellular growth was determined. For the selective index (SI), the value was calculated by comparing the IC_{50} value of $Cu(SBCM)_2$ in MCF-10A cell line against the IC_{50} value of $Cu(SBCM)_2$ in MCF-7 cancer cell lines.[9]

2.5 Morphological study

MCF-7 cells were seeded in 6-well plates at 1.3×10^5 cells per well in 3 mL of complete growth medium, followed by incubation at 37 °C (5% CO_2 and 95% air) for 24 hours and treated with $Cu(SMCM)_2$. Control cells treated with 0.3% DMSO alone were also included. The morphological changes were observed and the images were captured under an inverted light microscope (Olympus, PA, USA) at 0, 24, 48 and 72 hours. The same spot of cells was marked and captured.

2.6 Confirmation of apoptosis by Annexin V/PI flow cytometry assay

MCF-7 cells were seeded in a 25 cm^2 culture flask with a population of 300 000 cells and incubated overnight. Cells were then treated with $Cu(SBCM)_2$ at 20, 30 and 40 μM. Control cells (0.3% of DMSO as negative control and 10% DMSO as positive control) were also included in this experiment. After 48 hours, cells were washed twice with PBS (phosphate buffer saline) and were later detached by trypsinisation. Cold PBS was then used to wash cells and cells were re-suspended in 500 μL of 1× binding buffer (cell concentration 1×10^6 cells per mL). Next, 5 μL of Annexin-V-FITC and 5 μL of PI (propidium iodide) were added to cells. Cells were gently vortexed, incubated on ice for 10 minutes and analysed by NovoCyte® flow cytometry (ACEA Biosciences, San Diego, CA).

2.7 Cell cycle analysis

MCF-7 cells were seeded in 25 cm^2 cell culture flasks with 300 000 cells per flask, which allowed for cells attachment overnight. Cells were subsequently treated with 20, 30 and 40 μM of $Cu(SBCM)_2$ and incubated at 37 °C for 48 hours. All attached and floating cells were washed with cold PBS, fixed gently in 70% cold ethanol and stored at −20 °C overnight. Cold PBS was used to wash cells, followed by cell staining with RNase and PI for 30 minutes to ease cell cycle detection. Cell cycle distribution was evaluated using NovoCyte® flow cytometry from ACEA Biosciences (San Diego, CA).

2.8 Western blot analysis

Western blot was performed according to the previous publication.[8] Briefly, 300 000 MCF-7 cells were seeded and treated with $Cu(SBCM)_2$ for 24 and 48 hours. The cells were then lysed with RIPA buffer. The protein was separated by gel electrophoresis and transferred to PVDF membrane. The membrane was then blocked with 3% bovine serum albumen and probed overnight with mouse anti-p53 (1 : 2000) and anti-beta actin (1 : 10 000). Next, the membrane was incubated with horseradish peroxidase-conjugated goat anti-mouse secondary antibodies (1 : 20 000) for 1 hour at room temperature. Detection was performed with Chemi Lumi-One L Detection Reagent and ChemiDoc MP System.

2.9 Determination of intracellular ROS in $Cu(SBCM)_2$-treated cells

MCF-7 and MDA-MB-231 breast cancer cells were seeded in 6-well plates at a density of 1.3×10^5 cells per well in 3 mL of complete growth culture media and incubated for 24 hours at a temperature of 37 °C under 5% CO_2 to allow attachment of cells. Next, the spent media were removed and the cells were pre-treated with 10 μM DCFH-DA in complete culture media for 1 hour. Upon the removal of excess DCFH-DA, the cells were washed with phosphate-buffered saline (PBS) twice and followed by treatment with hydrogen peroxide or $Cu(SBCM)_2$ in culture media for 30 minutes. 0.3% DMSO alone, as a negative control, was also used to treat the cells. The samples

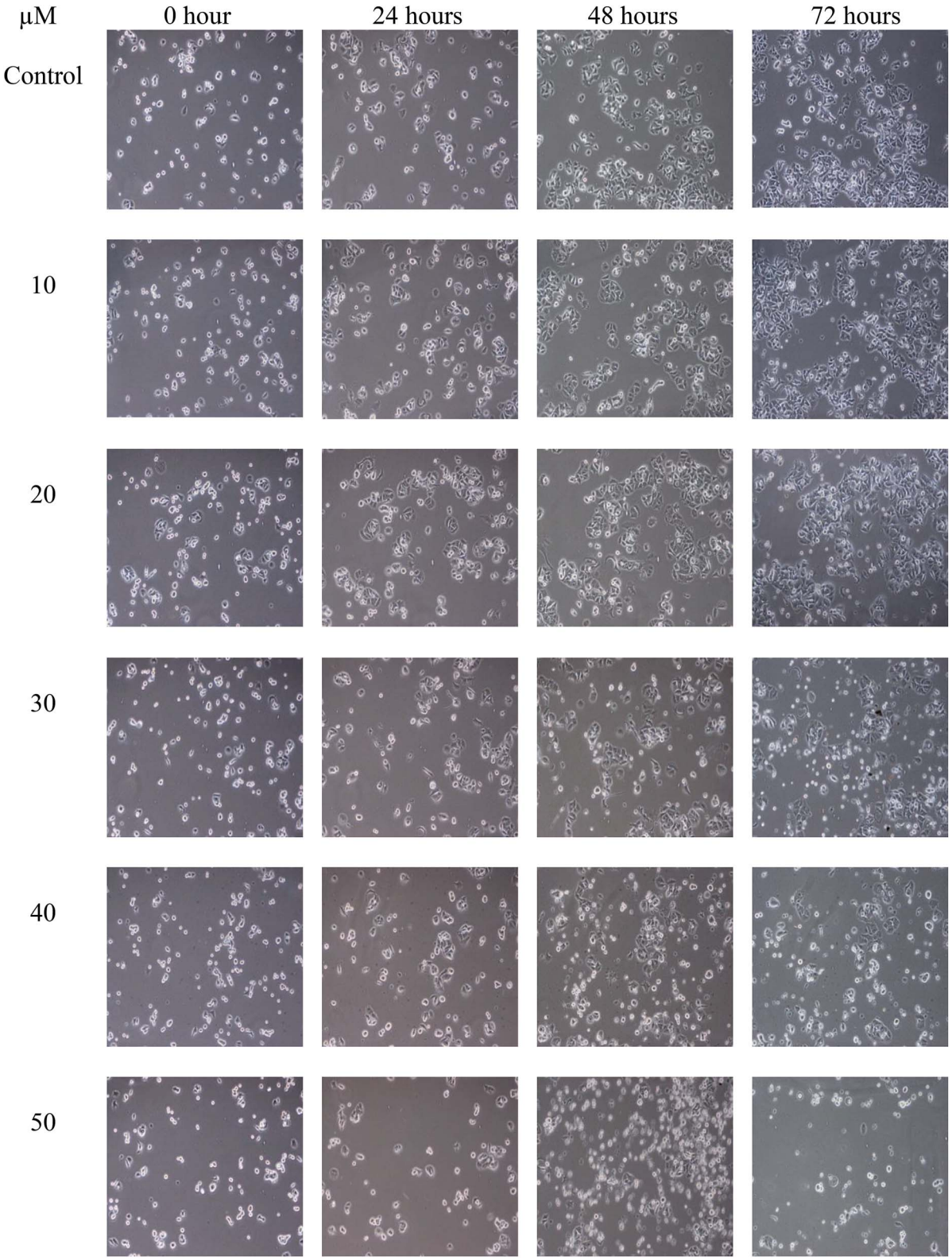

Fig. 3 The population of MCF-7 cells treated with $Cu(SBCM)_2$ as observed under inverted light microscope at the same spot for 72 hours (100×).

were then examined and images were captured using the Eclipse Ti2 inverted fluorescent microscope (Nikon, Shanghai, China) with excitation and emission wavelengths of 485 nm and 535 nm.

2.10 Evaluation of the effects of antioxidants on $Cu(SBCM)_2$-induced cell death in MCF-7

MCF-7 and MDA-MB-231 breast cancer cells were seeded in 96-well plates at a density of 5000 cells per well and incubated at

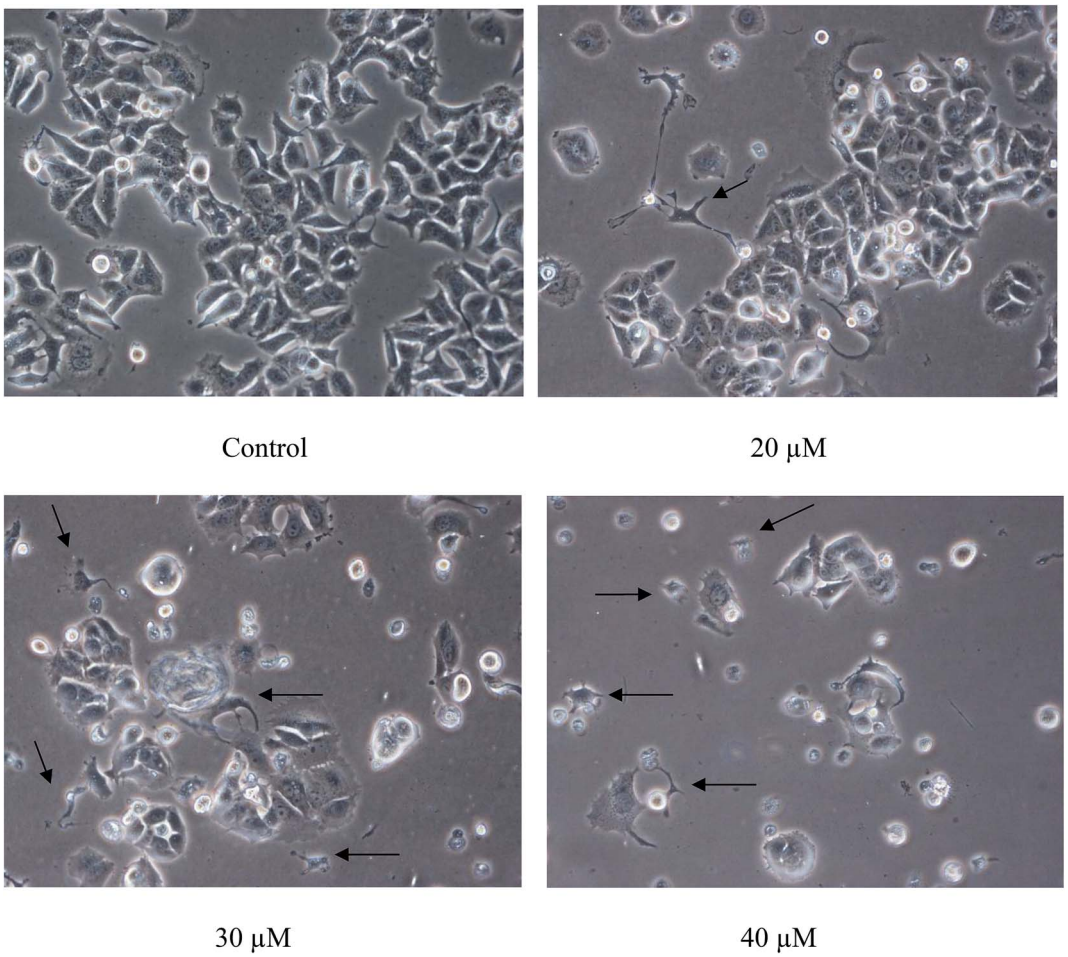

Fig. 4 Close-up view of MCF-7 cells treated with $Cu(SBCM)_2$ at 48 hours (200×). Cellular shrinkage was observed in $Cu(SBCM)_2$-treated MCF-7 cells (arrows).

a temperature of 37 °C under 5% CO_2 and 95% air for 24 hours. Following cell attachment, cells were treated with doxorubicin or $Cu(SBCM)_2$ or co-treated with 100 μM α-tocopherol or 100 μM *N*-acetylcysteine (NAC) for 48 hours. Each well was then added with 20 μL MTT (5 mg mL^{-1} in PBS) and followed by incubation for 3 hours. Next, the extra MTT was removed by aspiration and the purple formazan crystals formed were dissolved in 200 μL of DMSO. The cell viability, which was proportional to the amount of formazan crystals formed, was determined by measuring the absorbance at 570 nm and at background of 630 nm (reference wavelength) by employing ELx800™ Absorbance Microplate Reader (BioTek Instruments Inc., Vermont, USA). Cell viability was calculated by using formula as mentioned above and a graph of percentage of cell viability against $Cu(SBCM)_2$ concentration were plotted from the experiments.

2.11 Molecular docking studies

To explore the interactions of $Cu(SBCM)_2$ with various biological macromolecules, we performed docking studies of $Cu(SBCM)_2$ with DNA (PDB code 1BNA), DNA topoisomerase I (PDB code 1SC7), and human ribonucleotide reductase (PDB code 4X3V). All three targets have previously been shown to potentially account for the antitumor activity of thiosemicarbazone metal complexes.[10,11]

The metal complex was first constructed using ChemDraw 17 and subjected to geometry optimisation using the AM1 force-field. The target structures were downloaded from the Protein Data Bank and prepared using the Protein Preparation module implemented in Schrodinger Maestro.[12] Hydrogen atoms were added, missing side chains were modelled using Prime,[13] appropriate protonation states were assigned at pH 7, and hydrogen bond networks were optimised. The target structures were then subjected to restrained energy minimisation before docking. Docking calculations were performed using Glide SP,[14] with the Induced Fit Protocol used for protein targets to allow for side chain flexibility.[15] Default settings were used. The docking grid was centred on the major and minor groove for DNA or the co-crystallized ligand for DNA topoisomerase I and ribonucleotide reductase respectively. A total of 20 binding poses were initially generated for each target, with the final pose chosen based on the docking score and comparison with the co-crystallised ligands.

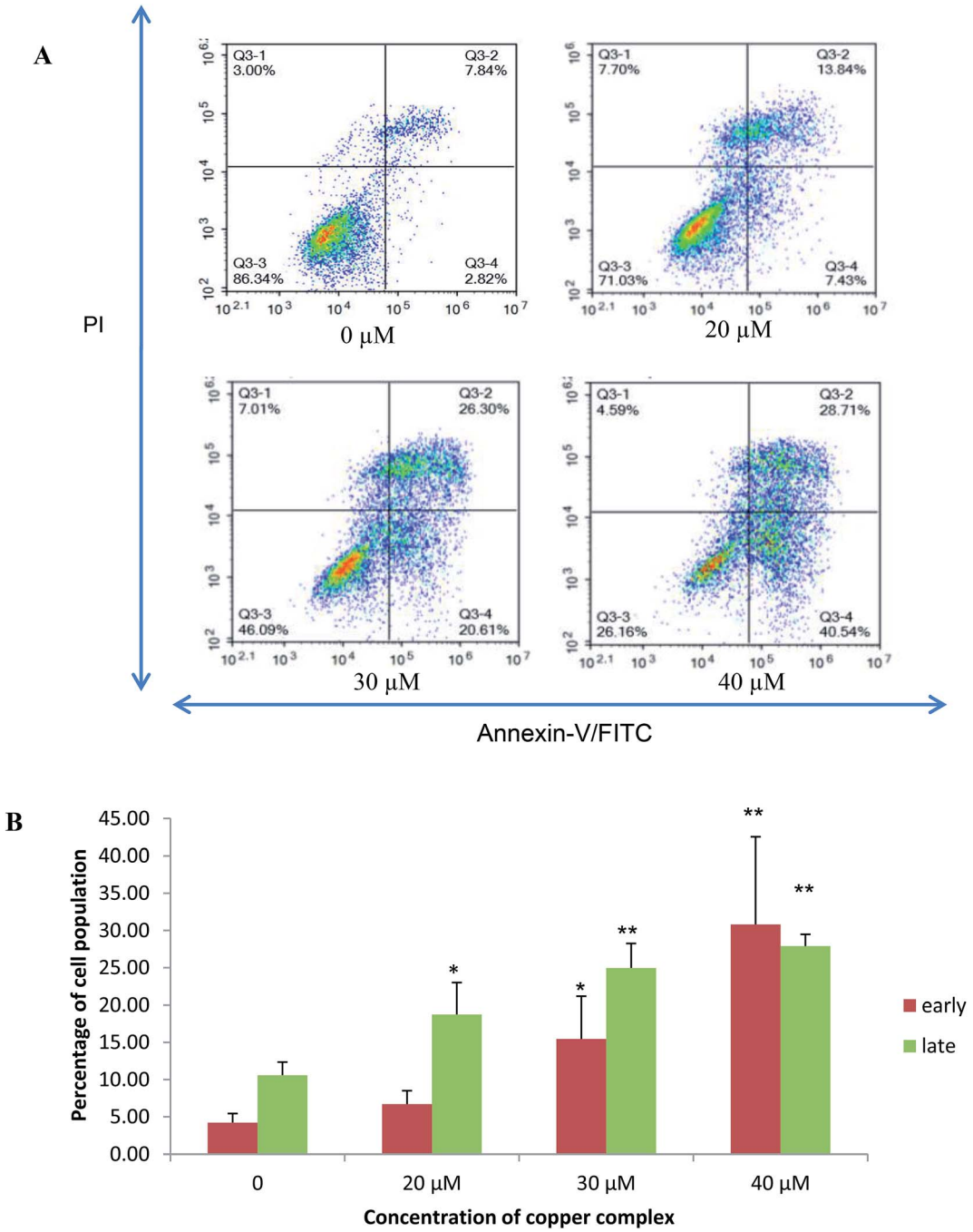

Fig. 5 Annexin-V/-FITC/PI Flow cytometry analysis of MCF-7 breast cancer cells treated with 20, 30 and 40 μM of $Cu(SBCM)_2$ for 48 hours. (A) These figures are from representative experiments carried out at least two independent test. The viable cells, early apoptotic and necrotic/secondary necrotic cells was represented by the lower left quadrant (Annexin-V^-/PI^-), lower right (Annexin-V^+/PI^-) and upper (Annexin-V^+/PI^+) quadrant, respectively. (B) Percentage of early and late apoptotic cells after $Cu(SBCM)_2$ administration in MCF-7 cells. Data were mean ± SD of two independent experiments. (* indicates $p < 0.05$ when compared with control, ** indicates $p < 0.001$ when compared with control).

2.12 Statistical analysis

Statistical analysis was conducted using the Statistical Package for Social Science (SPSS) version 21.0. Data were expressed as mean ± standard deviation (mean ± SD). Results were analysed by one-way analysis of variance (ANOVA), followed by Dunnett's *post hoc* test. A difference is considered to be significant at $p < 0.05$.

3. Results

3.1 $Cu(SBCM)_2$ inhibited the growth of MCF-7 cells but less toxic towards MCF-10A

The growth of MCF-7 cells was not inhibited by SBCM up to 60 μM as compared to control. However, treatment with $Cu(SBCM)_2$ significantly inhibited ($p < 0.05$) the growth of MCF-

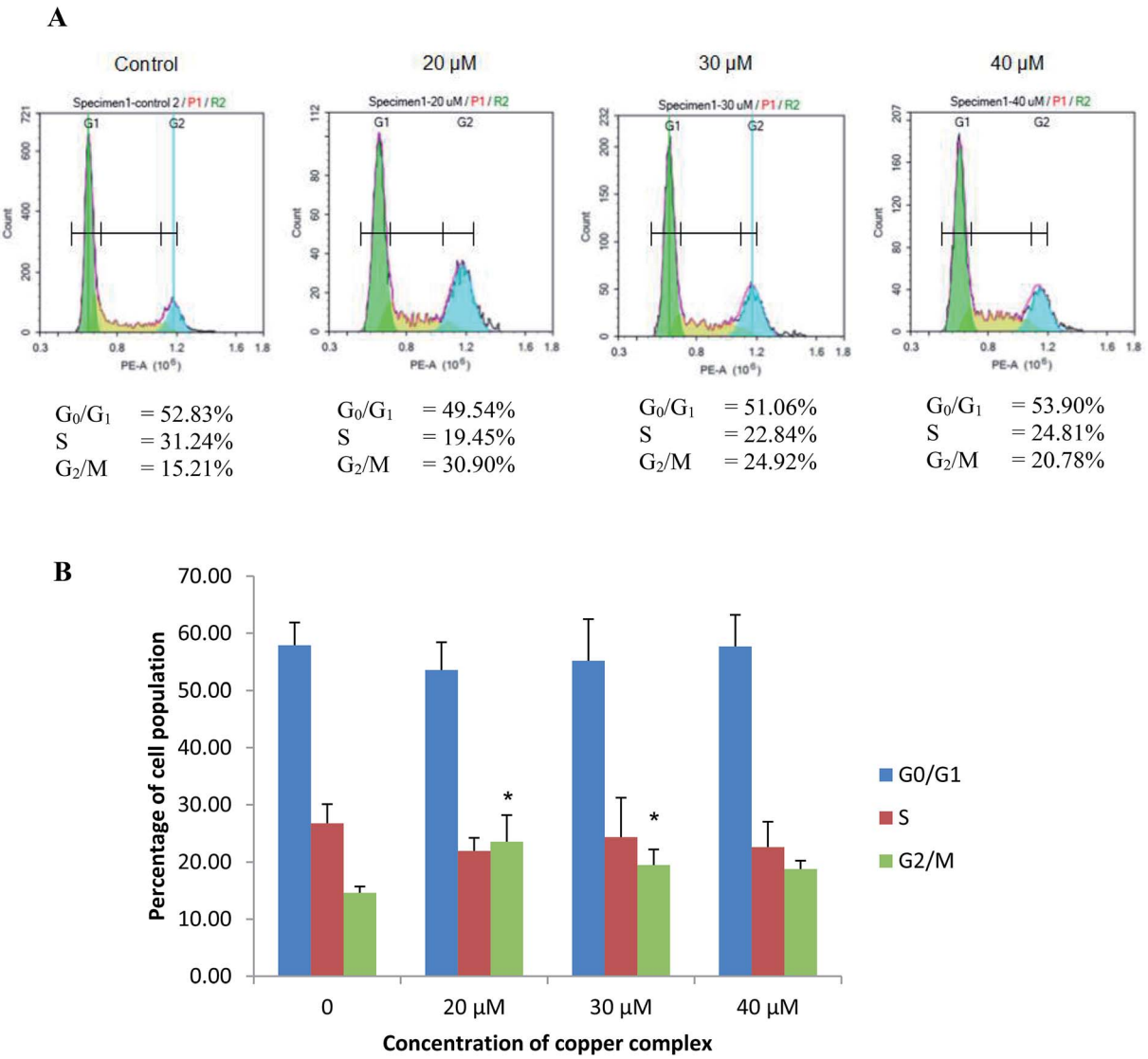

Fig. 6 Flow cytometry analysis of MCF-7 breast cancer cells treated with 20, 30 and 40 μM of $Cu(SBCM)_2$ for 48 hours. (A) Representative figures of cell cycle distribution (G_0/G_1, S, and G_2/M) showing accumulation of $Cu(SBCM)_2$-treated cells in G_2/M stage. Results shown are one of the two independent experiments conducted. (B) Bar chart showing accumulation of MCF-7 breast cancer cells in each cell cycle phase after $Cu(SBCM)_2$ administration. Data were mean ± SD of two independent experiments. (* indicates $p < 0.05$ when compared with control).

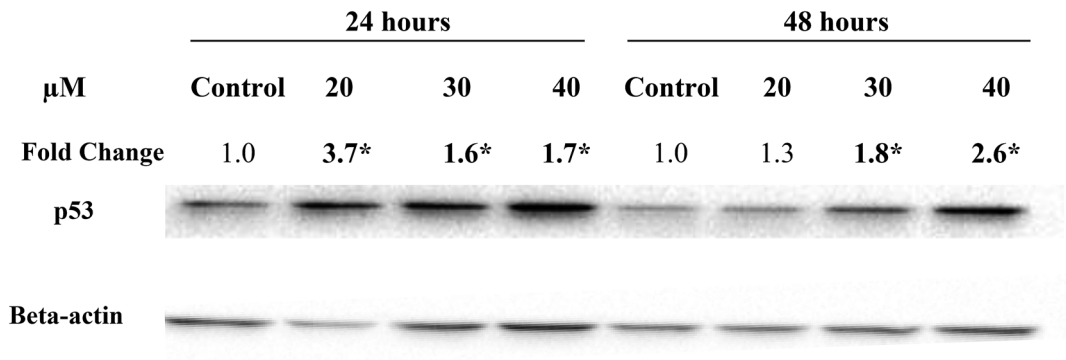

Fig. 7 Expression levels of wild-type p53 protein in MCF-7 cells following treatment with $Cu(SBCM)_2$. Fold change was normalised against beta-actin and compared to the control. Each data point represents the mean of three independent experiments ± SD. * significantly different from the control ($p < 0.05$).

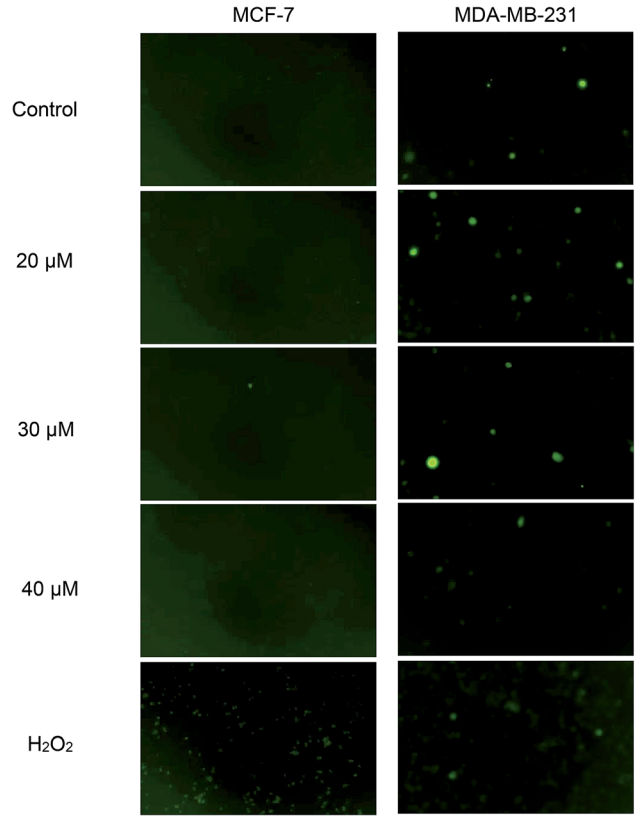

Fig. 8 Effects of $Cu(SBCM)_2$ on the production of ROS in breast cancer cells. After pretreatment with 10 μM DCFDA for 1 hour, cells were treated with $Cu(SBCM)_2$ for 30 minutes and examined under fluorescence microscope. Green fluorescence indicates the presence of intracellular ROS.

7 cells in a dose-dependent manner (Fig. 2A). The growth of MCF-7 cells appeared to be completely inhibited at approximately 27 μM and cell death was observed at higher concentration of $Cu(SBCM)_2$.

The viability of MCF-7 cells treated with 20, 30 and 40 μM of $Cu(SBCM)_2$ decreased to 65.0 ± 2.5%, 53.1 ± 5.3% and 42.3 ± 5.%, respectively as compared to control. As for non-cancerous MCF-10A breast cells, similar trend was observed. Nevertheless, the viability of MCF-10A cells was 81.8 ± 2.8%, 79.0 ± 11.3% and 69.9 ± 4.5% for concentrations 20, 30 and 40 μM, respectively, in which the viabilities were significantly higher than the one in MCF-7 cancer cell lines (Fig. 2B). The IC_{50} value of $Cu(SBCM)_2$ towards MCF-7 and MCF-10A were 32 and 60 μM, respectively, at 48 hours. The calculated selective index of $Cu(SBCM)_2$ in MCF-7 is 1.9, indicating that $Cu(SBCM)_2$ is more selective towards cancer cells than non-cancerous cells.

3.2 $Cu(SBCM)_2$ induced apoptosis towards MCF-7 cells

The population of attached cells in the control, 10 μM and 20 μM increased from 0 to 72 hours. For the cells treated with $Cu(SBCM)_2$ at higher concentration, increased in the cell population was noted until 24 hours and the cells detached from the substratum (Fig. 3). $Cu(SBCM)_2$-treated MCF-7 cells demonstrated characteristics of apoptosis such as cellular shrinkage at 48 hours. Nevertheless, other features of apoptosis such as chromatin condensation and formation of apoptotic bodies were not observed (Fig. 4). To confirm our observation that $Cu(SBCM)_2$ induced apoptosis towards MCF-7 cells, the $Cu(SBCM)_2$-treated-MCF-7 cells were then stained with Annexin V-FITC/PI and analysed using flow cytometry. Results indicated (Fig. 5A and B) that cells underwent early and late apoptosis. The percentage of early apoptosis cells treated with $Cu(SBCM)_2$ at 20, 30 and 40 μM was 6.70 ± 1.81%, 15.45 ± 5.72% and 30.79 ± 11.75%, respectively, in comparison to control (4.22 ± 1.23%). Similar trend was also noted for late apoptosis population. The percentage of late apoptosis cells treated with $Cu(SBCM)_2$ at 20, 30 and 40 μM was 18.74 ± 4.26%, 24.95 ± 3.30% and 27.88 ± 1.60%, respectively, in comparison to control (10.59 ± 1.77%).

3.3 $Cu(SBCM)_2$ induced G_2/M cell cycle arrest in MCF-7 breast cancer cells

MCF-7 cells treated with 20, 30 and 40 μM of $Cu(SBCM)_2$ resulted in a drop in S phase population from 26.73 ± 3.36% to 21.94 ± 2.31%, 24.36 ± 6.87% and 22.62 ± 4.40%, respectively (Fig. 6). On the other hand, there was increments in G_2/M phase in comparison to control in which the percentage was increased from 14.60 ± 1.12% to 23.57 ± 4.61%, 19.47 ± 2.75% and 18.77 ± 1.47% at 20, 30 and 40 μM of $Cu(SBCM)_2$, respectively.

3.4 $Cu(SBCM)_2$ up-regulated p53 protein in MCF-7 cells

In the present study, treatment of MCF-7 cells with 20, 30 and 40 μM of $Cu(SBCM)_2$ for 24 hours significantly up-regulated the expression of wild-type p53 by 3.7, 1.6 and 1.7 folds, respectively. Similar trend was also observed when the cells were treated for 48 hours (Fig. 7).

3.5 Effects of $Cu(SBCM)_2$ on the intracellular ROS levels

Green fluorescence cell indicates the presence of intracellular ROS and the intensity increases with the levels of intracellular ROS. From Fig. 8, green fluorescence can be clearly seen in positive control (H_2O_2) of both cell lines. This indicates that H_2O_2 was able to induce ROS formation in both cell lines and subsequently, detected by DCFH-DA. Nonetheless, when both cell lines were exposed to concentrations of 20, 30 and 40 μM of $Cu(SBCM)_2$ for 30 minutes, there was no increased intensity in green fluorescence for both cell lines, as compared to the control.

3.6 NAC enhanced the cytotoxicity of $Cu(SBCM)_2$ in MCF-7 cells

Viability of MCF-7 cells after treatment with $Cu(SBCM)_2$ alone at 20 μM, 30 μM and 40 μM for 48 hours was 55%, 53% and 42%, respectively. Co-treatment of MCF-7 cells with 100 μM NAC and $Cu(SBCM)_2$ significantly decreased the cell viability to 29%, 33% and 24% (Fig. 9A). In contrast, co-treatment of MDA-MB-231 cells with antioxidants and $Cu(SBCM)_2$ did not affect the cell viability as compared to $Cu(SBCM)_2$ alone (Fig. 9B).

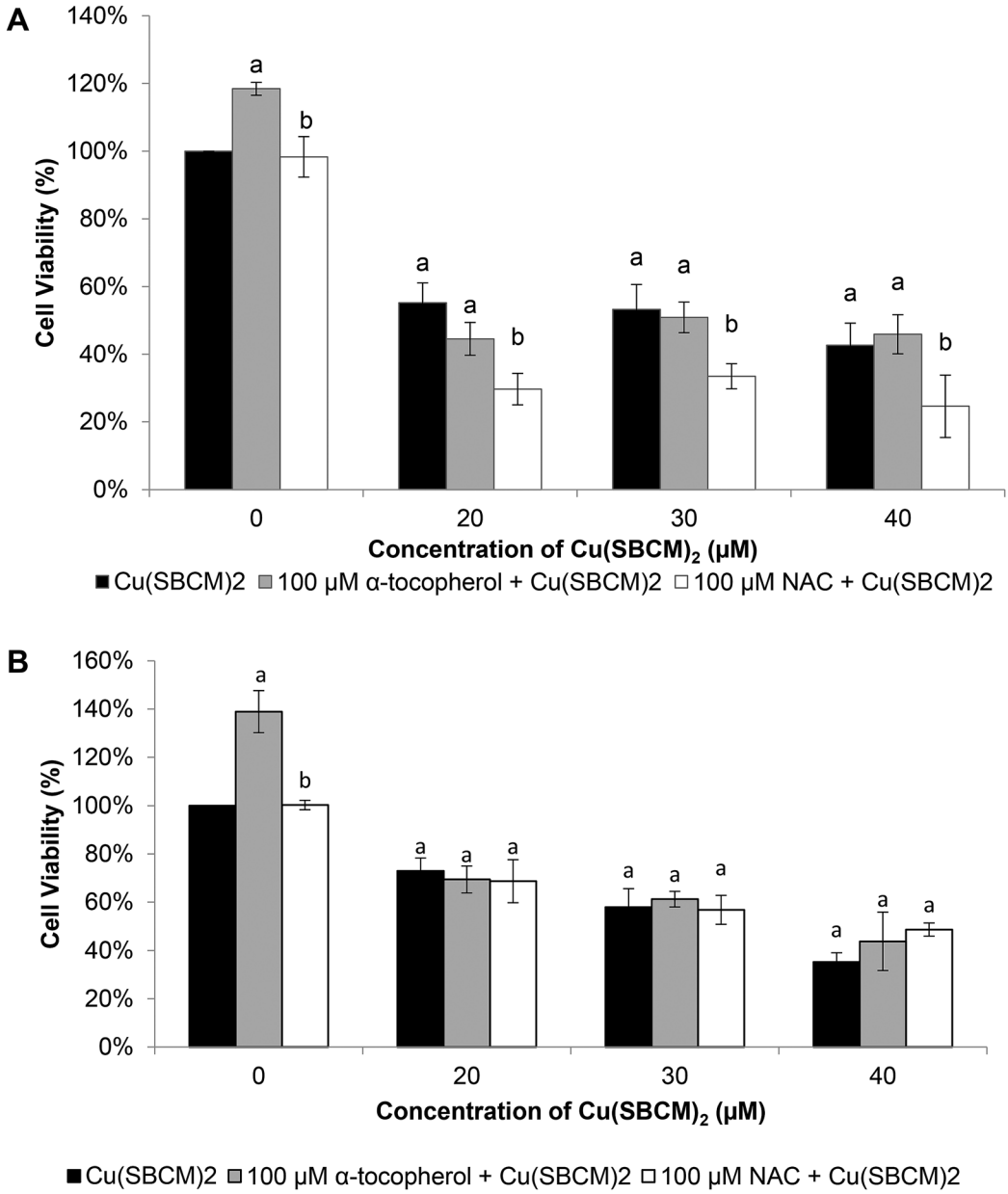

Fig. 9 Effects of antioxidants on the cytotoxicity of $Cu(SBCM)_2$. (A) and (B) represent the percentage of viability of MCF-7 and MDA-MB-231 cells after treatment with $Cu(SBCM)_2$ and α-tocopherol or NAC for 48 hours. Each data point represents the mean of triplicates ± SD. a and b in the same concentration were considered significantly difference ($p < 0.05$).

3.7 $Cu(SBCM)_2$ has a good binding towards DNA topoisomerase I

Of the three targets investigated, $Cu(SBCM)_2$ showed the greatest affinity for DNA topoisomerase I with a calculated binding free energy of -12.04 kcal mol^{-1}. This was in comparison to a calculated binding free energy of -7.52 kcal mol^{-1} for ribonucleotide reductase and -5.22 kcal mol^{-1} for DNA. We then performed the molecular docking in reference to MJ238, which is a known DNA topoisomerase I inhibitor that was co-crystallised in the 1SC7 crystal structure (Fig. 10A). The predicted binding free energy of $Cu(SBCM)_2$ towards DNA topoisomerase I (-12.04 kcal mol^{-1}) is lower than the predicted binding free energy of MJ238 towards DNA topoisomerase I (-8.22 kcal mol^{-1}), indicating that our $Cu(SBCM)_2$ binds stronger to the target. Molecular docking also revealed that $Cu(SBCM)_2$ intercalates the DNA base pair whenever the DNA is unwind (Fig. 10B). The key interaction in $Cu(SBCM)_2$ binding to DNA topoisomerase I is demonstrated in Fig. 10C.

4. Discussion

In the present study, SBCM-H Schiff base did not inhibit the growth of MCF-7 breast cancer cells. However, the conjugation of SBCM-H with copper [$Cu(SBCM)_2$] enhanced the inhibitory properties of the Schiff base towards MCF-7 breast cancer cells,

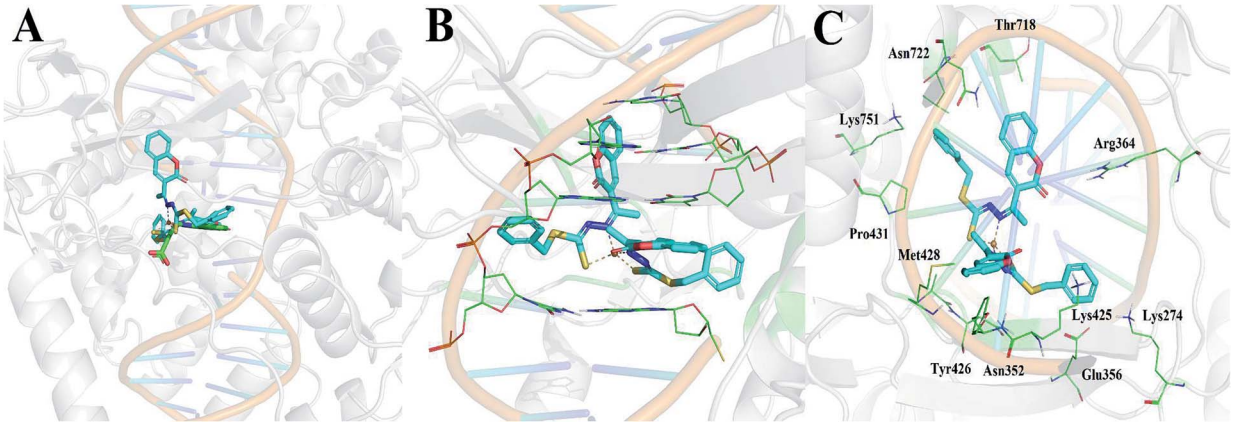

Fig. 10 (A) Binding of $Cu(SBCM)_2$ (cyan) in comparison to the co-crystallised DNA topoisomerase inhibitor MJ238 (green). (B) Intercalation of $Cu(SBCM)_2$ with base pairs. (C) Key interactions in $Cu(SBCM)_2$ binding to DNA topoisomerase I.

probably due to the increased uptake of Schiff base by the cells (Fig. 2A). Apart from that, $Cu(SBCM)_2$ was also evaluated towards non-cancerous MCF-10A breast cells. It was noted that $Cu(SBCM)_2$ demonstrated stronger inhibition towards MCF-7 than MCF-10A (Fig. 2B), suggesting that $Cu(SBCM)_2$ is more toxic towards cancer cells but less toxic towards normal cells. This warrants the safety profile of $Cu(SBCM)_2$ for future drug development.

Observation of cells under an inverted light microscope revealed that $Cu(SBCM)_2$ inhibited the growth (Fig. 3) and apoptosis (Fig. 4) towards MCF-7 breast cancer cells. Cells treated with $Cu(SBCM)_2$ showed cellular shrinkage (Fig. 4) postulating that $Cu(SBCM)_2$ induced apoptosis in MCF-7 cells, which was then further confirmed by Annexin-V/PI flow cytometry analysis (Fig. 5). Some other features of apoptosis such as membrane blebbing, chromatin condensation, nuclear fragmentation and formation of apoptotic bodies were not seen in MCF-7 cells under the inverted light microscope after treatment of $Cu(SBCM)_2$ due to caspase-3 deficiency in the MCF-7 cells. Caspase-3 is important for typical biochemical and morphological changes of cells undergoing apoptosis such as DNA nuclear fragmentation.[16] Since $Cu(SBCM)_2$ induced apoptosis in the caspase-3-deficient-MCF-7 cells, it is suggested that the induction of apoptosis *via* caspase-3-independent pathways. Although the exact mechanism of apoptosis in MCF-7 breast cancer cells is yet to be determined, but there are many different mechanisms of apoptosis that could possibly be induced by $Cu(SBCM)_2$ towards MCF-7 breast cancer cells.[17]

Apart from apoptosis, $Cu(SBCM)_2$ was also found to induce G_2/M phase cell cycle arrest towards MCF-7 breast cancer cells (Fig. 6). The induction of apoptosis and cell cycle arrest are very likely due to the increased expression of wild-type p53 by $Cu(SBCM)_2$ in MCF-7 cells (Fig. 7). Apoptosis may be induced by either p53-dependent or p53-independent pathways.[18] In the present study, the wild-type p53 of MCF-7 cells was significantly up-regulated by 20, 30 and 40 μM of $Cu(SBCM)_2$ suggesting the involvement of p53 pathway in $Cu(SBCM)_2$ induced apoptosis. In response to a stress signal, p53 up-regulation may result in extensive apoptosis.[19] The significantly increased expression levels of wild-type p53 in $Cu(SBCM)_2$-treated-MCF-7 cells indicating that $Cu(SBCM)_2$ is a stressor that induces p53 accumulation which in turn induces apoptosis in the MCF-7 cells.

$Cu(SBCM)_2$ exhibited a high redox potential which might be related to its cytotoxic effects.[7] The high redox potential demonstrated by $Cu(SBCM)_2$ suggests that in the $Cu(SBCM)_2$ complex, Cu(II) is easily reduced to Cu(I). Cu(I) has been recognised to take part in Fenton-like reactions that generate ROS which can subsequently cause damage to functional biomolecules, such as protein, lipids, DNA and RNA in the cells.[20] This proposes that the cytotoxicity of $Cu(SBCM)_2$ could be due to the production of intracellular ROS as copper complex of other variants have found that they induced cell death by induction of high oxidative stress.[21–25] Unexpectedly, based on the DCFH-DA assay results (Fig. 8), $Cu(SBCM)_2$ did not increase the ROS production in both MCF-7 and MDA-MB-231 cells. However, further exploration is required as DCFH-DA is not sensitive to all types of reactive species. Hence, there is a possibility that the cytotoxic effect of $Cu(SBCM)_2$ towards both cell lines was induced by reactive species that cannot be detected by DCFH-DA such as H_2O_2, reactive nitrogen species, $O_2^{\bullet-}$, and lipid peroxides.[26,27] This requires further investigation and confirmation.

To assess the role of ROS in the cytotoxicity of $Cu(SBCM)_2$, we co-treated the cancer cells with antioxidants. Surprisingly, instead of blocking the reduction in cell viability, NAC synergise the inhibition effect of $Cu(SBCM)_2$ towards MCF-7 cells but had no influence on the viability of MDA-MB-231 treated with $Cu(SBCM)_2$ (Fig. 9). Breast cancer is a heterogeneous disease and each breast cancer subtype is responsive towards different anticancer therapy. Different response towards the co-treatment with $Cu(SBCM)_2$ and α-tocopherol or NAC between MCF-7 and MDA-MB-231 breast cancer cell lines suggesting a new approach for the treatment of oestrogen receptor positive breast cancer. However, the mechanism of the synergistic anticancer effects between the antioxidants and $Cu(SBCM)_2$ is yet to be established. Similar results was reported in which co-incubation of NAC enhanced the killing effects of their copper complexes towards cancer cells and they proposed that thiol-induced redox

cycling of Cu(II) complex happens outside the cells. Upon the reduction of Cu(II) to Cu(I) by NAC, the Cu(I) complex forms H_2O_2 readily by dismutation of O_2^- in the extracellular fluid. H_2O_2 then diffuses into the cells where more ROS formation is induced.[28]

Our molecular docking studies indicated that DNA topoisomerase I may be the most likely target that accounts for the antitumor activity shown by $Cu(SBCM)_2$. The predicted binding mode of $Cu(SBCM)_2$ to DNA topoisomerase I was found to be remarkably similar to the co-crystallised indenoisoquinoline MJ238 (Fig. 10A),[29] whereby the ligand intercalates at the site of DNA cleavage between the +1 and −1 base pairs through π–π stacking with the coumarin moiety (Fig. 10B). While the predicted binding mode of $Cu(SBCM)_2$ lacks the bidentate interaction of MJ238 with the two nitrogens on the Arg364 side chain, it is stabilised by an additional π–π stacking interaction between the phenyl ring and the cystosine base (Fig. 10C). While experimental validation will be needed to confirm these findings, they provide a useful starting point to further explore potential structure–activity relationships.

5. Conclusion

$Cu(SBCM)_2$ induced cell cycle arrest and apoptosis in caspase-3 deficient MCF-7 breast cancer cells possibly *via* the activation of wild-type p53 with less toxic towards non-cancerous MCF-10A cells. Antioxidants seems enhanced the cytotoxicity of $Cu(SBCM)_2$ towards MCF-7 cells. DNA topoisomerase I may be the most likely target that accounts for the antitumor activity shown by $Cu(SBCM)_2$. Based on our previously published and current data, $Cu(SBCM)_2$ has a great potential to be developed to target the breast cancer cells.

Author contributions

JBF, YST, CWH and LSY contributed to the design of the study and interpretation of data. LSY allowed us to use laboratory facilities for present study. MLL synthesised and characterized the copper complex. For data acquisition, JBF, JHL, YZL and LSN contributed to the MTT assay, morphological study and Western blot analysis. LSN, PXT, CYB, SWL and LCC contributed to Flow cytometry and ROS study. JSEL performed the molecular docking study. This manuscript is prepared and critically revised by JBF, YST, CWH and LSY.

Conflicts of interest

The authors declare that they have no conflict of interest.

Acknowledgements

The present work was financially supported by MAHSA Research Grant (RP89-02/16) and Taylor's University Internal Research Grant Scheme (TRGS/ERFS/1/2018/SBS/034). Special thanks are delivered to the Laboratory of Vaccine and Immunotherapeutics, Institute of Bioscience and Virology Lab 1, Faculty of Biotechnology and Biomolecular Sciences from Universiti Putra Malaysia for their support and assistance in completing this study.

References

1 Y. Ichikawa, M. Ghanefar, M. Bayeva, R. Wu, A. Khechaduri, S. V. N. Prasad, R. K. Mutharasan, T. J. Naik and H. Ardehali, *J. Clin. Invest.*, 2014, **124**, 617–630.
2 H. H. Wong, C. Barton, G. Acton, R. McLeod and S. Halford, *Eur. J. Cancer*, 2016, **66**, 9–16.
3 R. Jasmine and S. A. Kumar, *Indian J. Pharmacol.*, 2016, **48**, 99–100.
4 S. Kaushik, H. Shyam, R. Sharma and A. K. Balapure, *Indian J. Pharmacol.*, 2016, **48**, 637–642.
5 C. Davies, H. Pan, J. Godwin, R. Gray, R. Arriagada, V. Raina, M. Abraham, V. H. Medeiros Alencar, A. Badran, X. Bonfill, J. Bradbury, M. Clarke, R. Collins, S. R. Davis, A. Delmestri, J. F. Forbes, P. Haddad, M.-F. Hou, M. Inbar, H. Khaled, J. Kielanowska, W.-H. Kwan, B. S. Mathew, I. Mittra, B. Müller, A. Nicolucci, O. Peralta, F. Pernas, L. Petruzelka, T. Pienkowski, R. Radhika, B. Rajan, M. T. Rubach, S. Tort, G. Urrútia, M. Valentini, Y. Wang, R. Peto and Adjuvant Tamoxifen: Longer Against Shorter (ATLAS) Collaborative Group, *Lancet*, 2013, **381**, 805–816.
6 H. Xie and Y. J. Kang, *Curr. Med. Chem.*, 2009, **16**, 1304–1314.
7 M. L. Low, G. Paulus, P. Dorlet, R. Guillot, R. Rosli, N. Delsuc, K. A. Crouse and C. Policar, *BioMetals*, 2015, **28**, 553–566.
8 J. B. Foo, M. L. Low, J. H. Lim, Y. Z. Lor, R. Z. Abidin, V. E. Dam, N. A. Rahman, C. Y. Beh, L. C. Chan, C. W. How, Y. S. Tor and L. S. Yazan, *BioMetals*, 2018, **31**, 505–515.
9 O. A. Peña-Morán, M. L. Villarreal, L. Álvarez-Berber, A. Meneses-Acosta and V. Rodríguez-López, *Molecules*, 2016, **21**, 1013.
10 F. A. Beckford, A. Brock, A. Gonzalez-Sarrías and N. P. Seeram, *J. Mol. Struct.*, 2016, **1121**, 156–166.
11 J. Haribabu, K. Jeyalakshmi, Y. Arun, N. S. P. Bhuvanesh, P. T. Perumal and R. Karvembu, *RSC Adv.*, 2015, **5**, 46031–46049.
12 *Maestro*, Schrödinger, LLC, New York, 2016.
13 M. P. Jacobson, D. L. Pincus, C. S. Rapp, T. J. F. Day, B. Honig, D. E. Shaw and R. A. Friesner, *Proteins: Struct., Funct., Bioinf.*, 2004, **55**, 351–367.
14 R. A. Friesner, J. L. Banks, R. B. Murphy, T. A. Halgren, J. J. Klicic, D. T. Mainz, M. P. Repasky, E. H. Knoll, M. Shelley, J. K. Perry, D. E. Shaw, P. Francis and P. S. Shenkin, *J. Med. Chem.*, 2004, **47**, 1739–1749.
15 W. Sherman, T. Day, M. P. Jacobson, R. A. Friesner and R. Farid, *J. Med. Chem.*, 2006, **49**, 534–553.
16 R. U. Jänicke, *Breast Cancer Res. Treat.*, 2009, **117**, 219–221.
17 J. Yuan and H. R. Horvitz, *Cell*, 2004, **116**, S53–S56.
18 L. M. McNamee and M. H. Brodsky, *Genetics*, 2009, **182**, 423–435.
19 Z. Wang and Y. Sun, *Transl. Oncol.*, 2010, **3**, 1–12.
20 P. J. Jansson, P. C. Sharpe, P. V. Bernhardt and D. R. Richardson, *J. Med. Chem.*, 2010, **53**, 5759–5769.

21 M. Hajrezaie, M. Paydar, S. Zorofchian Moghadamtousi, P. Hassandarvish, N. S. Gwaram, M. Zahedifard, E. Rouhollahi, H. Karimian, C. Y. Looi, H. M. Ali, N. Abdul Majid and M. A. Abdulla, *Sci. World J.*, 2014, **2014**, 1–12.
22 V. F. S. Pape, D. Türk, P. Szabó, M. Wiese, E. A. Enyedy and G. Szakács, *J. Inorg. Biochem.*, 2015, **144**, 18–30.
23 A. A. Recio Despaigne, J. G. Da Silva, P. R. da Costa, R. G. Dos Santos and H. Beraldo, *Molecules*, 2014, **19**, 17202–17220.
24 A. Sîrbu, O. Palamarciuc, M. V. Babak, J. M. Lim, K. Ohui, E. A. Enyedy, S. Shova, D. Darvasiová, P. Rapta, W. H. Ang and V. B. Arion, *Dalton Trans.*, 2017, **46**, 3833–3847.
25 A. Subastri, A. Suyavaran, E. Preedia Babu, S. Nithyananthan, R. Barathidasan and C. Thirunavukkarasu, *J. Cell. Physiol.*, 2018, **233**, 1775–1790.
26 B. Halliwell and M. Whiteman, *Br. J. Pharmacol.*, 2004, **142**, 231–255.
27 Y. S. Tor, L. S. Yazan, J. B. Foo, A. Wibowo, N. Ismail, Y. K. Cheah, R. Abdullah, M. Ismail, I. S. Ismail and S. K. Yeap, *PLoS One*, 2015, **10**, e0127441.
28 C. R. Kowol, P. Heffeter, W. Miklos, L. Gille, R. Trondl, L. Cappellacci, W. Berger and B. K. Keppler, *J. Biol. Inorg Chem.*, 2012, **17**, 409–423.
29 B. L. Staker, M. D. Feese, M. Cushman, Y. Pommier, D. Zembower, L. Stewart and A. B. Burgin, *J. Med. Chem.*, 2005, **48**, 2336–2345.